Eur. Phys. J. D **12**, 117–122 (2000)

THE EUROPEAN PHYSICAL JOURNAL D

EDP Sciences

Pressure dependence of the Mg $3s4s^3S_1 \rightarrow 3s3p^3P_{0,1,2}$ transition in superfluid ^{4}He

I. Baumann[a], A. Breidenassel, C. Zühlke, A. Kasimov, G. zu Putlitz, I. Reinhard[b], and K. Jungmann[c]

Physikalisches Institut der Universität Heidelberg, Philosophenweg 12, 69120 Heidelberg, Germany

Received 18 February 2000

Abstract. The pressure shifts of the $3s4s^3S_1 \rightarrow 3s3p^3P_{0,1,2}$ transition of magnesium atoms immersed in superfluid helium have been measured at (1.3 ± 0.1) K between saturated vapour pressure and 24 bar. The wavelength is blue shifted linearly by (0.07 ± 0.01) nm/bar. This value can be satisfactorily described in the framework of the standard bubble model.

PACS. 67.40.Yv Impurities and other defects – 32.50.+d Fluorescence, phosphorescence (including quenching) – 32.70.Jz Line shapes, widths, and shifts

1 Introduction

Superfluid helium is a quantum substance with unique features, like the phenomenon of superfluidity or the unusual dispersion curve [1]. Despite a successful history and expanded research in this field important properties of this quantum liquid remain still unexplained.

Different experimental methods have been employed so far to study superfluid helium. In general, they can be divided into two groups of conceptually distinguishable approaches. Firstly, the superfluid itself is under investigation, which means parameters like its density, its friction or its phase diagram are measured. Secondly, the interaction of probe particles with the quantum fluid can be studied, *e.g.* the dispersion curve has been measured with neutron scattering. This group comprises experiments, where the experimental signal is derived from internal degrees of freedom of the microscopic probes. Foreign atoms and ions can be implanted and the changes in their spectra reveal information about the interactions of the probes with the helium environment [2–4]. In the experiment reported here magnesium atoms are introduced into the bulk superfluid and electronic transitions within them are observed.

Foreign atoms or ions generally perturb the helium environment. Depending on the interaction between the probe particles and the superfluid helium distinctly different defect structures are formed. If the density around the foreign particle is lowered compared to the unperturbed helium bulk a void with the foreign atom in its center forms; such structures are known as bubbles. They are determined by the interplay of repulsive and attractive interactions, the Pauli repulsion between the electrons of the probe and the helium atoms surrounding it, as well as the volume, respectively the surface energy of the bubble. In contrast, there may be a strongly increased density, even larger than the solidification density. These objects have been named snowballs. They originate mainly from the very strong attractive polarization forces between the foreign particle and the surrounding liquid and are typically observed for positively charged particles, particularly for most of the positive ions due to strong monopole induced dipole interactions [2–4, 7].

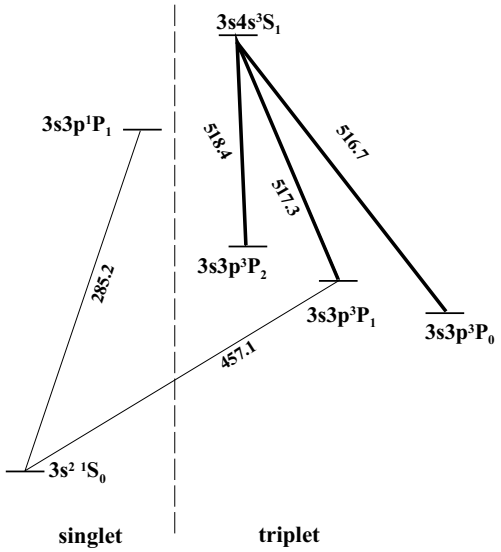

Fig. 1. Energy level diagram of the triplet and singlet states of magnesium atoms. The numbers at the electronic transitions are the free atomic wavelength in nm.

[a] *Present address*: The Boston Consulting Group GmbH & Partner, Kronprinzenstr. 28, 70173 Stuttgart, Germany.

[b] *Present address*: Gesellschaft für Schwerionenforschung, Planckstraße 1, 64291 Darmstadt, Germany.

[c] e-mail: `jungmann@physi.uni-heidelberg.de`

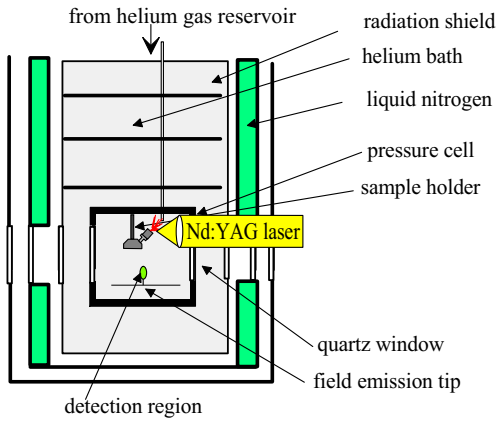

Fig. 2. Cross-section of the lower part of the helium bath cryostat. The pressure cell is mounted inside the liquid helium bath. Magnesium ions are produced by laser ablation, drawn by an electric field towards the bottom of the cell, where they recombine with electrons released from a field emission tip.

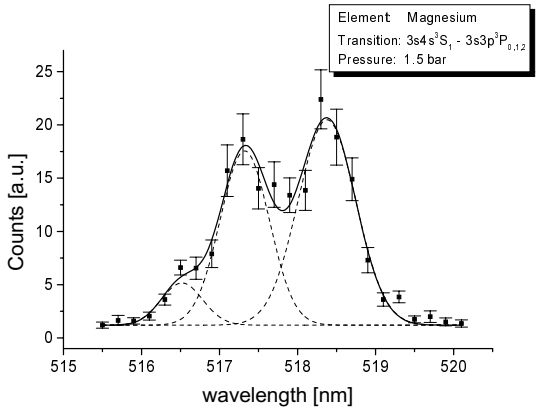

Fig. 3. Recombination spectrum of the $3s4s\,^3\mathrm{S}_1 \rightarrow 3s3p\,^3\mathrm{P}_{0,1,2}$ transition measured at an increased helium pressure of 1.5 bar.

From spectroscopy measurements [8] it is known that magnesium atoms form bubble like structures under saturated vapour pressure. As a surprising feature magnesium atoms show in liquid helium an unusual three times longer lifetime for the $3s3p\,^3\mathrm{P}_1 \rightarrow 3s^2\,^1\mathrm{S}_0$ intercombination transition compared to this transition in vacuum [8]. For other systems such a behaviour has not been as pronounced as in this case. Therefore atomic magnesium has been chosen to study the influence of an increased helium pressure on a bubble-like structure in order to investigate whether this object is stable at higher helium pressures and may even undergo observable structure changes.

Due to the interaction of the magnesium atoms with the surrounding superfluid its electronic states are perturbed and the emission as well as the absorption lines of corresponding electronic transitions are shifted with respect to their vacuum values. Further they are broadened and have asymmetric shapes [4]. The wavelength of the electronic transitions and the mean bubble size can be predicted in the framework of a straightforward theoretical approach, the standard bubble model. This is based on macroscopic quantities such as surface and volume energies [9]. It has been successfully applied to singlet and doublet states so far [4–6]. Here it is employed to describe triplet states as well.

2 Experimental set-up

A copper pressure cell (inner volume = 600 cm^3) is mounted inside a helium bath cryostat (see Fig. 2). Its temperature is maintained between 1.2 and 1.4 K. The cell is connected with a helium gas reservoir *via* a capillary system (inner diameter = 1.5 mm) to allow filling by condensation of helium gas. The liquid pressure can be adjusted by applying a corresponding helium pressure from the gas reservoir. Optical access to the cell is possible through three quartz windows (diameter = 39 mm) which are sealed by indium gaskets up to 40 bar helium pressure at 1.2 K.

In the experiment the sample material under investigation has a typical size of $5 \times 5 \times 5$ mm. Ions are produced by laser ablation from the surface of the sample with a focused Nd:YAG laser (focal diameter 4.4 μm). The laser energy is 8 mJ per pulse with a pulse width of 6−8 ns at wavelength 1064 nm [10]. The ions are drawn by an electric field towards the bottom of the experimental chamber, where most of them recombine with electrons from a field emission tip. The tip voltage was varied between −0.9 and −2.8 kV and the probe voltage between 0.6 and 1.2 kV. These voltages were adjusted for each pressure to maximize the signal to noise ratio. These parameters correspond to electric fields between 0.4 and 1.0 kV/cm for a drift length of 42 mm. The light emitted from the electron cascade after recombination is imaged onto the entrance of a grating monochromator (Czerny-Turner type) with a wavelength resolution of 0.025 nm. A photomultiplier tube (EMI S 20 extended) serves as detector, the signal of which is digitized and recorded time resolved in 400 bins of a width of 1.0 ms.

The recombination method as well as the implantation and production of ions directly in the liquid based on the use of laser ablation are both well established techniques [4]. In this experiment they were combined for the first time. Experimental data were taken at pressures in the full accessible pressure range of the experimental method up to 24 bars, where close to the solidification point the ion mobility drops dramatically with increasing pressure. A typical spectrum of the $3s4s\,^3\mathrm{S}_1 \rightarrow 3s3p\,^3\mathrm{P}_{0,1,2}$ transition at a helium pressure of 1.5 bar is displayed in Figure 3. The mean wavelength of the three emission lines can be obtained by a fit of three overlapping Gaussian line shapes.

3 Calculation of the emission wavelength with the standard bubble model

The bubble model allows a prediction of the bubble size as well as of the energy shift of electronic transitions compared with the free atomic case.

The total energy of the defect E_{tot} is the sum of two terms, the electronic contribution of the free atom E_{free} and the so called defect energy E_{defect} [9]:

$$E_{\mathrm{tot}} = E_{\mathrm{defect}} + E_{\mathrm{free}} = E_{\mathrm{bubble}} + E_{\mathrm{int}} + E_{\mathrm{free}}. \quad (1)$$

The defect part includes the bubble energy E_{bubble} which is needed to form the void and the pairwise interaction E_{int} between the defect atom and surrounding helium atoms. The bubble energy consists of macroscopic terms like volume E_{vol}, surface E_{surf} and volume kinetic E_{vk} energies where the later is due to the helium density gradient at the bubble surface [9,11]:

$$\begin{aligned} E_{\mathrm{bubble}} &= E_{\mathrm{vol}} + E_{\mathrm{surf}} + E_{\mathrm{vk}} \quad (2)\\ &= \frac{4\pi}{3} p R_{\mathrm{B}}^3 (R_0) + 4\pi\sigma R_{\mathrm{B}}^2 (R_0) \\ &\quad + \frac{\hbar^2}{8 m_{\mathrm{He}}} \int_0^\infty \frac{(\nabla\rho(r, R_0, \alpha))^2}{\rho(r, R_0, \alpha)}\, \mathrm{d}^3 r \quad (3) \end{aligned}$$

with the helium pressure p, the equilibrium bubble radius R_{B}, the radius R_0 where the liquid density approaches zero, the width of the transition region from the bubble to the helium environment $1/\alpha$, the surface density σ and the density $\rho(r, R_0, \alpha)$. The density follows an assumed parametrization [11]:

$$\rho = \begin{cases} 0 & r < R_0 \\ \rho_0 \left[1 - [1 + \alpha\,(r - R_0)]\, \mathrm{e}^{-\alpha(r - R_0)}\right] & r \geq R_0 \end{cases} \quad (4)$$

with the constant helium density $\rho_0 = 0.15$ g/cm^3. This ansatz assumes that helium is incompressible as $\rho(r, R_0, \alpha)$ can't be larger than ρ_0. The bubble model has been successfully applied to describe experiments at elevated helium pressures, *e.g.* for electron bubbles the pressure dependence of electronic transitions can be very well calculated [12]. Further, there is a less than 20% change in ρ_0 [13] over the whole pressure range covered in this experiment and the associated relative difference in the calculated pressure shift, which arises from the last term in equation (3), is below 2×10^{-3}. Therefore we find the assumption of the incompressibility of the bulk helium as a motivation in our case.

The defect energy is obtained by adding the interaction energy E_{int} of the states involved and the bubble energy. Multi particle interactions are neglected in this approach and only pairwise magnesium-helium interactions are taken into account [14]:

$$E_{\mathrm{int}}(S) = 4\pi \int_0^\infty V_S(r)\, \rho(r, R_0, \alpha)\, r^2\, \mathrm{d}r \quad (5)$$

$$\begin{aligned} E_{\mathrm{int}}(P) = 4\pi \int_0^\pi \sin\theta\, \mathrm{d}\theta \int_0^\infty &[(\cos\theta)^2 V_P^\sigma(r) \\ &+ (\sin\theta)^2 V_P^\pi(r)] \rho(r, R_0, \alpha)\, r^2 \mathrm{d}r \quad (6) \end{aligned}$$

[4] with the interatomic pair potentials V_S, V_P^σ, V_P^π, where S stands for s-states and P for p-states, which are in the case of magnesium atoms in triplet p-states only known without fine structure splitting [15]. The fine structure splitting arising from spin-orbit interactions is assumed not to depend on the externally applied helium pressure, therefore a prediction for all three emission lines can be made.

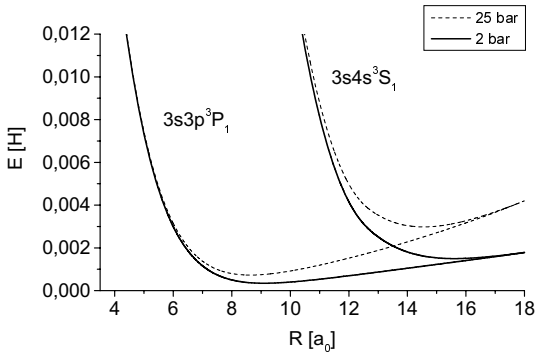

Fig. 4. Defect energy of the triplet states $3s4s\,^3\mathrm{S}_1$ and $3s3p\,^3\mathrm{P}_1$ of the magnesium atom as a function of the internuclear magnesium-helium-distance R in units of hartree (1 H = 27.212 eV) calculated by use of the bubble model (with $\alpha = 1.18 a_0^{-1}$, $a_0 = 0.529 \times 10^{-10}$ m). The dashed line corresponds to a pressure of 25 bar, the other one to a pressure of 2 bar.

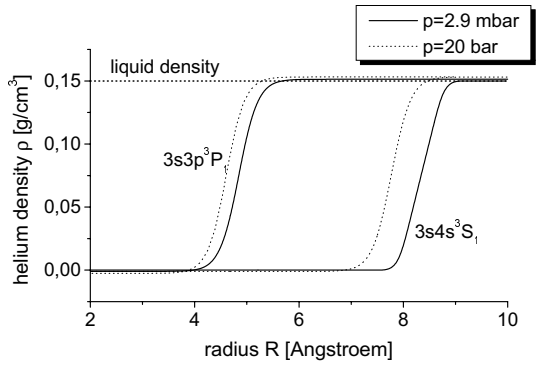

Fig. 5. Density distribution of the helium environment around a magnesium atom in the $3s3p\,^3\mathrm{P}_1$ state or in the $3s4s\,^3\mathrm{S}_1$ state at helium pressures of 2.9 mbar and 20 bar.

As the energy of the free atom is only an additive contribution to the total energy, it can be neglected for the calculation of the radial dependence of the defect energy, but has to be added for the calculation of the wavelength of the electronic transitions. An example of the calculated defect energies of the two interesting states $3s4s\,^3\mathrm{S}_1$ and $3s3p\,^3\mathrm{P}_1$ for two different helium pressures (2 and 25 bar) is shown in Figure 4.

The radius at the minimum of the defect energy is the mean equilibrium radius of the defect structure in the specific state. It decreases with increasing pressure (see Fig. 5) for the $3s4s\,^3\mathrm{S}_1$ state from 8.34 Å at 2.9 mbar to 7.68 Å at 25 bar and for the $3s3p\,^3\mathrm{P}_1$ state from 4.85 Å to 4.56 Å. This decrease in the equilibrium radius with increasing pressure is qualitatively similar to the behaviour of an electron bubble at an enhanced helium pressure [12]. Additionally the model predicts the width of the transition

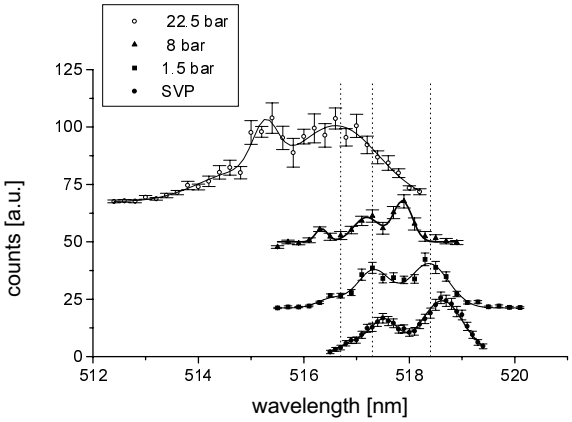

Fig. 6. Emission spectra of the $3s4s^3S_1 \rightarrow 3s3p^3P_{0,1,2}$ transition at different helium pressures (3 mbar, 1.5, 8 and 22.5 bar). The dashed lines correspond to the free atomic transitions.

region from the bubble to the helium environment to be 0.45 Å.

The sum of the free energy and the difference of the two defect state energies yields a prediction of the pressure dependent emission wavelength of the transition $3s4s^3S_1 \rightarrow 3s3p^3P_1$:

$$\lambda(p) = (516.48 \pm 0.01)[\text{nm}] - (0.08 \pm 0.01)\,[\text{nm/bar}]p\,[\text{bar}]. \quad (7)$$

The wavelength of the other two emission lines is obtained by adding the respective fine structure splitting (+1.1 nm for $^3P_0$, −0.53 nm for $^3P_2$) to the zero pressure wavelength of 516.48 nm.

4 Experimental results

Typical measured emission spectra for helium pressures 3 mbar, 1.5, 8 and 22 bar are shown in Figure 6. The values below 1 bar were measured with another experimental cell [10] as the pressure cell allows measurements only at helium pressures above 1 bar.

At saturated vapor pressure we find all three lines slightly red shifted (see Tab. 1) compared to the corresponding transitions observed in free atoms. The spectra shift with increasing pressure to smaller wavelength (blue shift), in accordance with the bubble model. The central emission wavelength of the three transitions is given in Figures 7, 8 and 9 as a function of the applied helium pressure. The error bars result from the line shape fits. The uncertainty of the wavelength calibration of the monochromator is 0.1 nm common to all points. The dotted line is the calculated wavelength predicted by the standard bubble model (see Sect. 3).

The pressure dependence of the three emission lines is:

- $3s4s^3S_1 \rightarrow 3s3p^3P_0$:
  $\lambda = (517.11 \pm 0.04)$ [nm] $-(0.09 \pm 0.01)$[nm/bar]p [bar],
- $3s4s^3S_1 \rightarrow 3s3p^3P_1$:
  $\lambda = (517.51 \pm 0.06)$ [nm] $-(0.06 \pm 0.01)$[nm/bar]p [bar],
- $3s4s^3S_1 \rightarrow 3s3p^3P_2$:
  $\lambda = (518.52 \pm 0.04)$ [nm] $-(0.06 \pm 0.01)$[nm/bar]p [bar].

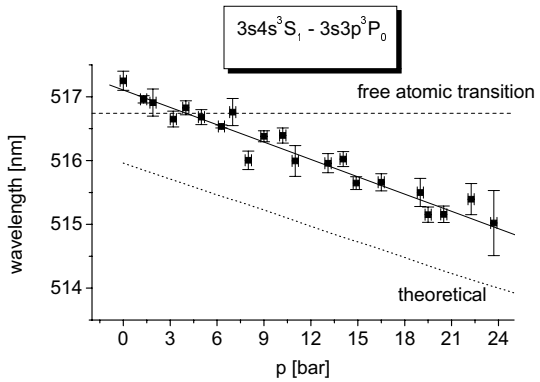

Fig. 7. Emission wavelength of the $3s4s^3S_1 \rightarrow 3s3p^3P_0$ transition of the magnesium atom as a function of the helium pressure. The dotted line corresponds to the emission wavelength calculated by use of the bubble model. The dashed line corresponds to the free atomic transition at 516.74 nm.

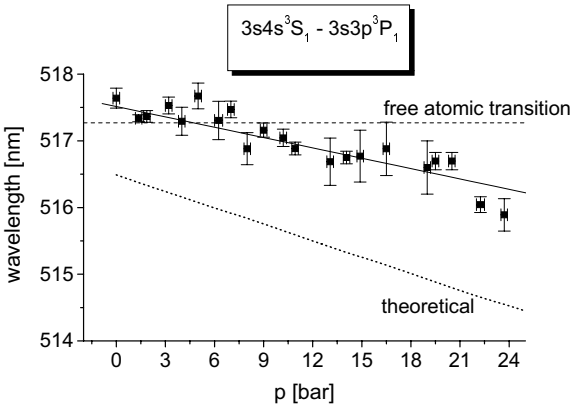

Fig. 8. Emission wavelength of the $3s4s^3S_1 \rightarrow 3s3p^3P_1$ transition of the magnesium atom as a function of the helium pressure. The dotted line corresponds to the emission wavelength calculated by use of the bubble model. The dashed line corresponds to the free atomic transition at 517.27 nm.

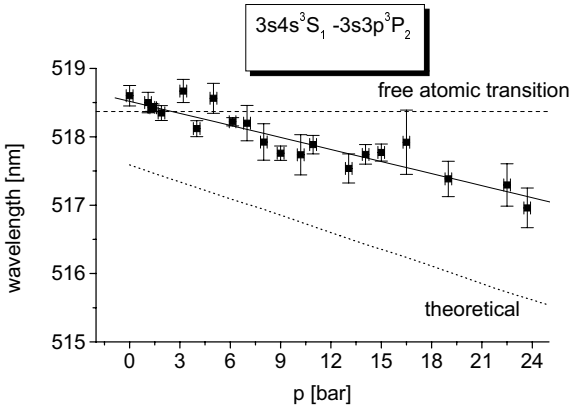

Fig. 9. Emission wavelength of the $3s4s^3S_1 \rightarrow 3s3p^3P_2$ transition of the magnesium atom as a function of the helium pressure. The dotted line corresponds to the wavelength calculated by use of the bubble model. The dashed line corresponds to the free atomic transition at 518.37 nm.

Table 1. Electronic transitions of various elements measured at an increased helium pressure. The table includes the free atomic transitions, the wavelength of the transitions in superfluid helium under saturated vapour pressure and the pressure line shifts. Also mentioned is the change of the wavelength because of a pressure increase relative to the wavelength of the transitions at saturated vapour pressure.

	transition	free atom [nm]	superfl. helium saturated vapor pressure [nm]	Refs.	superfl. helium increased pressure [nm/bar]	[%/bar]	Refs.
e^-	$1s$–$2p$		11270	[12]	61	0.541	[12,18]
	$1s$–$1p$		2480	[18]	252	10.161	
	$1s$–$1p$		2480	[18]	300	12.097	[19]
He_2	$2^3S \rightarrow 2^3P$	1083	1083.2	[20]	−0.11	−0.010	[21]
	$2^3P \rightarrow 2^3S$		1091.1		−0.3	−0.027	
Rb	$5^2S_{1/2} \rightarrow 5^2P_{1/2}$	794.76	777.96	[22]	−0.26	−0.033	[23]
Ba	$6s^{21}S_0 \rightarrow 6s6p^1P_1$	553.55	547.05	[24]	−0.11	−0.020	[25]
Cs	$6^2P_{1/2} \rightarrow 6^2S_{1/2}$	894.35	875.95	[22]	−0.26	−0.030	[26]
	$6^2S_{1/2} \rightarrow 6^2P_{1/2}$		892.25		−0.67	−0.075	
Tm	$4f^{12}\left(^3H_5\right)5d_{5/2}$	590.11	596.21				
	$6s^2\,(5,5/2)_{7/2}$ or $4f^{13}\left(^2F^0_{7/2}\right)6s6p\left(^3P^0_1\right)(7/2,1)_J$ $\rightarrow 4f^{13}\left(^2F^0_{5/2}\right)6s^2$	589.73	596.21	[27]	−0.06	−0.01	[27]
Mg	$3s4s\,^3S_1 \rightarrow 3s3p\,^3P_0$	516.73	517.11	this	$-(0.09 \pm 0.01)$	−0.017	this
	$3s4s\,^3S_1 \rightarrow 3s3p\,^3P_1$	517.27	517.51	work	$-(0.06 \pm 0.01)$	−0.012	work
	$3s4s\,^3S_1 \rightarrow 3s3p\,^3P_2$	518.36	518.52		$-(0.06 \pm 0.01)$	−0.012	

The deviation in wavelength between the theoretical and the experimental curves may be due in part to the precision of the pair potentials and is rather small compared to other calculations [16], *e.g.* for barium atoms in superfluid helium the deviation is about 14 nm [17]. In general, part of these small differences may also arise from the assumption of incompressible bulk material and from neglected bulk density variations in the vicinity of the defect. Further the concept of pair potentials excludes many body effects and in particular correlations of the electrons. The red shift of the lines at saturated vapour pressure is smaller than the difference between the calculated and the measured absolute values of the transition wavelengths. Therefore a quantitative explanation of this offset will require a refinement of the model employed here which successfully describes the line shift as a function of helium pressure.

The quality of the agreement of the calculated and measured pressure shifts for all three lines can be tested with a statistical hypothesis test, the Student test. The deviation of the three values is compatible with statistical fluctuations. Therefore a mean pressure line shift of (0.07±0.01 nm/bar) can be derived. This very good consistency between the experimental and the theoretical values allows the conclusion that the magnesium atoms seem to maintain a bubble like structures under increased helium pressures. The pressure shift is monotonous.

5 Discussion

As a consequence of the higher pressure the bubble like defect shrinks, *i.e.* the equilibrium radius decreases. The repulsive part of the pair potential energies due to Pauli forces rises in the upper S state already at larger radii than for the lower P state which implies a smaller wavelength for emitted radiation.

Up to now only few pressure dependent measurements of electronic transitions of foreign particles implanted into superfluid helium exist (see Tab. 1). A quantitative comparison between the published line shifts and the results presented in this paper is not possible for the line shift themselves, because different types of transitions have been investigated. Since the foreign atom-helium interaction potential are not comparable with each other, the different shifts for the various elements are not surprising. Interesting is a comparison concerning the relative pressure shift in wavelength which is much larger for the electron bubble than for any other structure. This reflects the fact that the electron bubble is much more compressible than the other bubbles. The similarity of the relative line shifts, *i.e.* the change of wavelength with pressure relative to the transition wavelength at saturated vapor pressure, for Mg, Rb, Ba, Tm and He_2 may be taken as indication that in all these cases bubbles are formed with similar size and compressibility. The within statistics linear behaviour of the pressure shifts suggests smooth and continuous change in the size and structure of the defect caused by all these systems.

This work was supported in part by the Deutsche Forschungsgemeinschaft (DFG). We would like to express our thanks to B. Tabbert and M. Foerste for their input at an early stage and their constant interest and suggestions. A.K. would like to acknowledge an Alexander von Humboldt postdoctoral fellowship.

References

1. D.G. Henshaw, A.D. Woods, Phys. Rev. **121**, 1266 (1961).
2. J.P. Toennies, A.F. Vilesov, Ann. Rev. Phys. Chem. **49**, 1 (1998) and references therein.
3. S.I. Kanorsky, A. Weis, Adv. At. Mol. Opt. Phys. **38**, 87 (1998) and references therein.
4. B. Tabbert, H. Günther, G. zu Putlitz, J. Low Temp. Phys. **5/6**, 653 (1997) and references therein.
5. T. Kinoshita, K. Fukuda, T. Matsuura, T. Yabuzadi, Phys. Rev. A **53**, 4054 (1996).
6. J. Dupont-Roc, Z. Phys. B **98**, 383 (1995).
7. K.R. Atkins, Phys. Rev. **116**, 1339 (1959).
8. H. Günther, M. Foerste, C. Hönninger, G. zu Putlitz, B. Tabbert, Z. Phys. B **98**, 395 (1995).
9. A.P. Hickman, W. Steets, N.F. Lane, Phys. Rev. B **12**, 3705 (1975).
10. I. Baumann, M. Foerste, K. Layer, G. zu Putlitz, B. Tabbert, Ch. Zühlke, J. Low Temp. Phys. **110**, 213 (1998).
11. A.P. Hickman, N.F. Lane, Phys. Rev. Lett. **26**, 1216 (1971).
12. C.C. Grimes, G. Adams, Phys. Rev. B **41**, 6366 (1990).
13. R.J. Donnelly, *Experimental Superfluidity*, edited by W.I. Glaberson, P.E. Parks (University of Chicago Press, Chicago, 1967), pp. 226-227.
14. M. Beau, Dissertation, University Heidelberg, 1990.
15. Q. Hui, Ph.D. thesis, Saitama University, 1997.
16. M. Foerste, I. Baumann, U. Pritzsche, G. zu Putlitz, B. Tabbert, J. Wiebe, C. Zühlke, Optical and mobility measurements of alkali earth atoms and ions in superfluid helium, *Advances in solid state physics* (B. Kramer, Friedr. Vieweg & Sohn, Braunschweig/Wiesbaden, 1999), pp. 355-367.
17. M. Foerste, Dissertation, University Heidelberg, 1997.
18. C.C. Grimes, G. Adams, Phys. Rev. B **45**, 2305 (1992).
19. A. Golov, Z. Phys. B **98**, 363 (1995).
20. J.C. Hill, O. Heybey, G.K. Walters, Phys. Rev. Lett. **26**, 1213 (1971).
21. F.J. Soley, W.A. Fitzsimmons, Phys. Rev. Lett. **32**, 988 (1974).
22. Y. Takahashi, K. Sano, T. Kinoshita, T. Yabuzaki, Phys. Rev. Lett. **71**, 1035 (1993).
23. T. Kinoshita, K. Fukada, Y. Takahashi, T. Yabuzaki, Phys. Rev. A **52**, 2707 (1995).
24. H. Bauer, M. Beau, B. Friedl, C. Marchand, K. Miltner, H.J. Reyher, Phys. Lett. A **146**, 134 (1990).
25. S. Kanorsky, A. Weis, M. Arndt, R. Dziewior, T.W. Hänsch, Z. Phys. B **98**, 371 (1995).
26. T. Kinoshita, K. Fukada, T. Yabuzaki, Z. Phys. B **98**, 387 (1995).
27. K. Ishikawa, A. Hatakeyama, K. Gosyono-o, S. Wada, Y. Takahashi, T. Yabuzaki, Phys. Rev. B **56**, 780 (1997).